Supporting Information for

New 2,2':6',2''-terpyridines as colorimetric and fluorescent censors for fluoride ions

Qian-Yong Cao,*[a] Ming Li,[a] Li Zhou,[a] and Zhong-Wei Wang*[b]

[a]Department of Chemistry, Nanchang University, Nanchang 330031, P. R. China. [b]College of Material Science and Technology, Shandong University of Science and Technology, Qingdao, 266590, P. R. China

Corresponding authors' e-mail: cqyong@ncu.edu.cn; wangzhongweif@fusilinchem.com

Experimental Section

General methods

Unless otherwise noted, materials were obtained from commercial suppliers and were used without further purification. Flash chromatography was carried out on silica gel (230-400 mesh). NMR spectra were recorded using Varian instruments (400MHz and 300 MHz). Chemical shifts were expressed in ppm and coupling constants (*J*) in Hz.

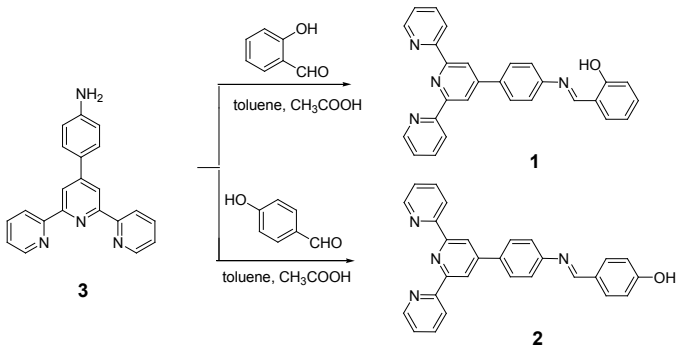

Scheme 1. Preparation route for **1** and **2**

Experimental Section

General methods

Unless otherwise noted, materials were obtained from commercial suppliers and were used without further purification. 4'-(4-Aminophenyl)-2,2':6',2''-terpyridine (**3**) was prepared by literature method. Flash chromatography was carried out on silica gel (230-400 mesh). NMR spectra were recorded using Varian instruments (400MHz and 300 MHz). Chemical shifts were expressed in ppm and coupling constants (*J*) in Hz.

Synthesis of 1

Under nitrogen, a solution of **3** (108mg, 0.33 mmol) and salicylaldehyde (0.2426 g, 2 mmol) in 30 ml dry toluene with some drops acetic acid as a catalyst was stirred under reflux for 24 h. Completion of the reaction was monitored through TLC for the disappearance of the starting compounds. Then the solvent was removed by evaporation under vacuum and the crude was purified by column chromatography (hexane/EA, 3:1, V/V) to yield **1** as a pale orange solid (69 mg, 49%). m.p.: 197-199 ^{o}C. ^{1}H NMR ($CDCl_3$, 400 MHz): δ 13.22 (OH, s, 1H), 8.77 (s, 2H)，8.75(d, J = 4.4 Hz, 2H), 8.70 (t, J = 7.6 Hz，3H), 8.01 (d, J = 8.4 Hz, 2H) , 7.90 (t, J=8.0 Hz, 2H) , 7.45 (m, 4H)，7.40 (t, J = 6.8 Hz, 2H), 7.07 (d, J = 4.0 Hz, 1H), 6.98 (t, J = 7.2 Hz, 1H). H NMR (DMSO-d_6, 400 MHz): δ 13.01 (OH, s, 1H), 9.09 (s, 1H), 8.74-8.80 (m, 4H)，8.69(d, J = 7.2 Hz, 2H), 8.05 (t, J = 6.8 Hz, 4H), 7.72 (d, J = 7.6 Hz, 1H) , 7.64 (d, J=4.0 Hz, 2H) , 7.55 (t, J=6.0 Hz, 2 H)，7.46 (t, J = 8.0 Hz, 1H), 6.98-7.04 (m, 2H). IR(KBr, cm^{-1}): 3434 cm^{-1}, 1620cm^{-1}. ^{13}C NMR ($CDCl_3$, 100 MHz): 163.0, 161.3, 156.2, 156.1, 149.3, 149.2, 137.0, 136.9, 133.4, 132.5, 128.5, 123.9, 121.8, 121.4, 119.2, 119.1, 118.6, 117.4 ppm. TOF-HR-MS $[M+1]^{+}$: 429.1711

Synthesis of 2

This compound was prepared in a similar way as **1** except that 4-hydroxybenzaldehyde was used in place of salicylaldehyde. Yield: 71%. m.p.: 235-237 ^{o}C. ^{1}H NMR ($CDCl_3$, 400 MHz): δ 8.76 (d, J = 4.8 Hz, 2H), 8.69 (d, J = 5.6 Hz, 4H), 8.40 (s, 1H), 7.92 (t, J = 8.0 Hz, 2H), 7.84 (d, J = 8.4 Hz, 2H), 7.76 (d, J = 7.6Hz,

2H)，7.40 (t，J = 6.0 Hz, 2H), 7.22(d, J = 8.0Hz, 2H), 7.03 (d, J = 8.4Hz, 2H). ^{1}H NMR (DMSO-d_6, 400 MHz): δ 10.21 (s, 1H), 8.78 (d, J = 4.0 Hz, 2H),8.75 (s, 2H), 8.69 (d, J = 8.0 Hz, 2H), 8.58 (s, 1H), 8.05 (t, J = 8.0 Hz, 2H), 7.98 (d, J = 8.4 Hz, 2H), 7.84 (d, J = 8.4 Hz, 2H), 7.54 (t, J = 6.0Hz, 2H)，7.43 (t，J = 8.4 Hz, 2H), 6.92 (d, J = 8.0Hz, 2H). ^{13}C NMR ($CDCl_3$, 100 MHz): 160.2, 156.4, 155.7, 153.1, 150.0, 149.0, 137.3, 135.1, 132.3, 131.1, 128.9, 124.0, 121.9, 121.4, 118.8, 116.3 ppm. IR (KBr, cm^{-1}): 3427cm^{-1}，1585cm^{-1}. TOF-HR-MS $[M+1]^{+}$: 429.1710.

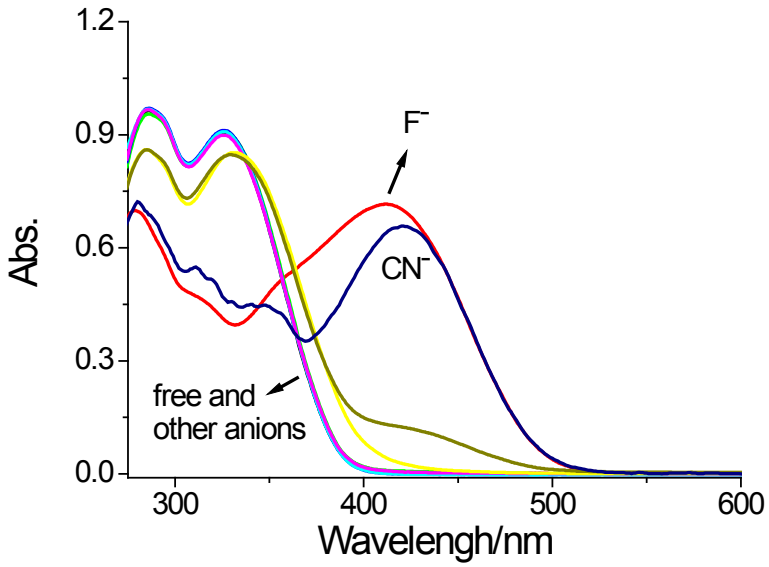

Fig. S1 UV-vis spectra of **2** (2×10^{-5}M) upon addition 20 equiv of anions in CH_3CN solution.

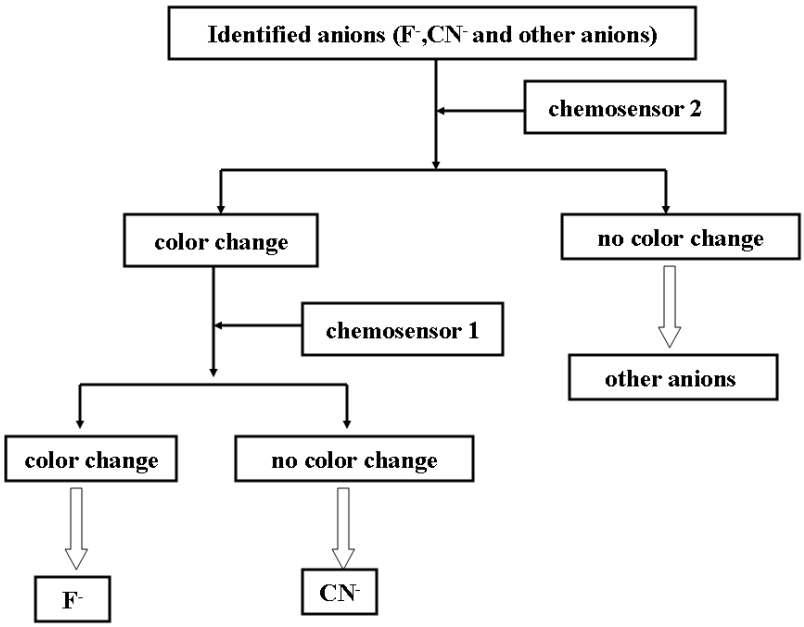

Fig. S2 Discrimination of F− and CN− from other anions with naked-eye observation by cooperative utilization of chemosensors **1** and **2**.

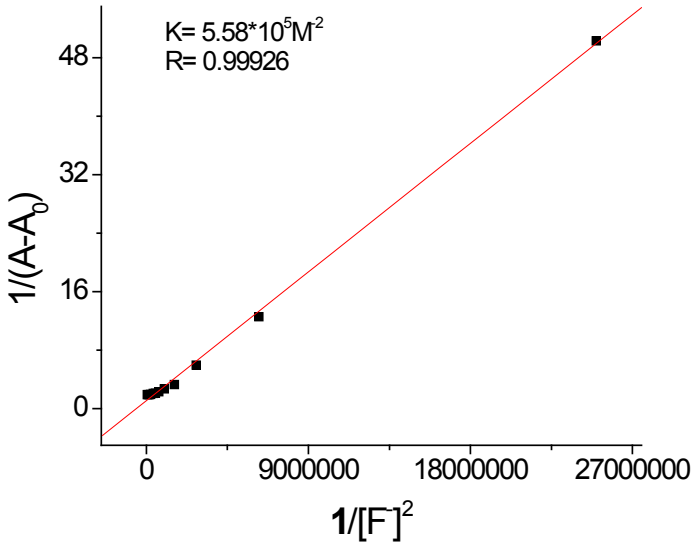

Fig. S3 Benesi-Hildebrand plot for 1:2 complex between **1** and F^-.

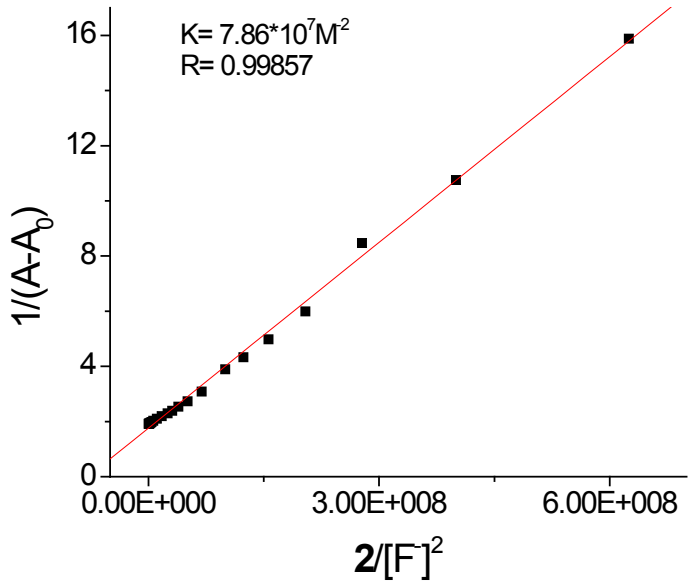

Fig. S4 Benesi-Hildebrand plot for 1:2 complex between **2** and F^-.

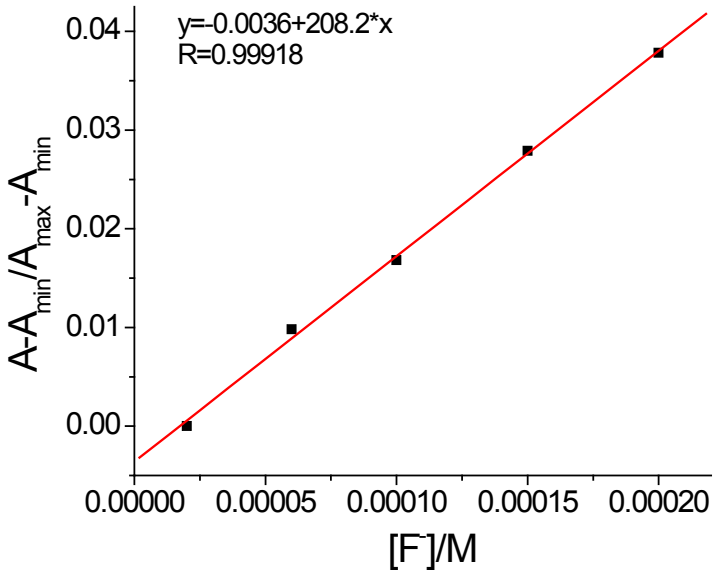

Fig. S5 Absorption of **1** in 438 nm upon the addition of different concentrations of F^- (0, 20, 60, 100, 150, 200 μM), normalized between the minimum absorption (0.0 μM F^-) and the maximum absorption intensity.

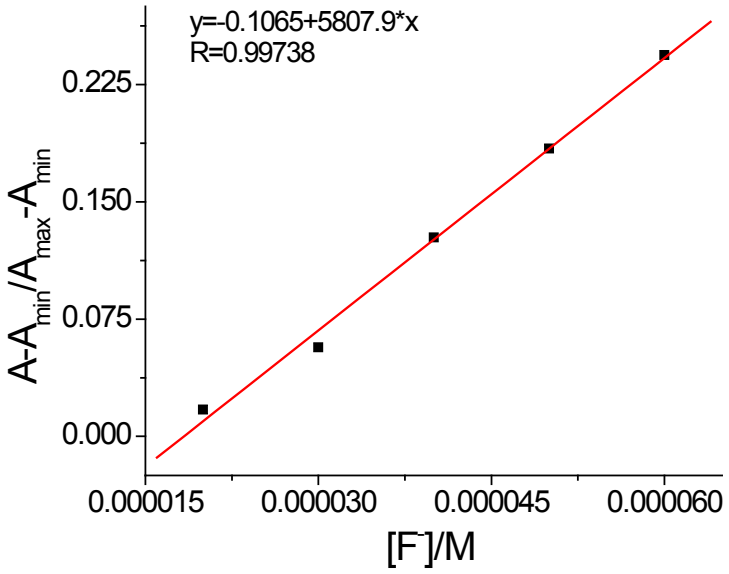

Fig. S6 Absorption of **2** in 415 nm upon the addition of different concentrations of F^- (0, 20, 30, 40, 50, 60 μM), normalized between the minimum absorption (0.0 μM F^-) and the maximum absorption.

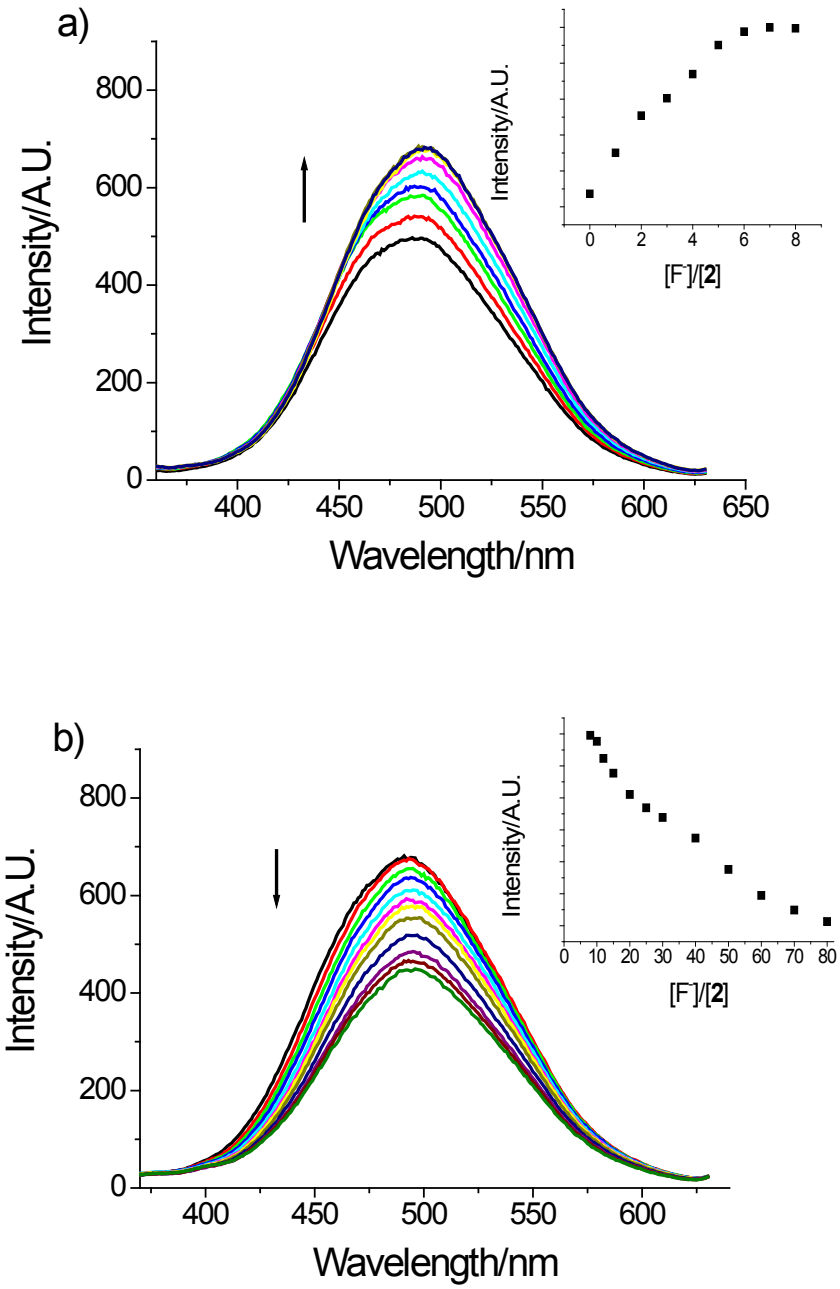

Fig. S7 Emission spectra of **2** upon the addition of 0-8 (a) and 8-80 equiv of F^- in CH_3CN solution (λ_{ex} = 330 nm). Inset: change in fluorescence intensity at 484 nm.

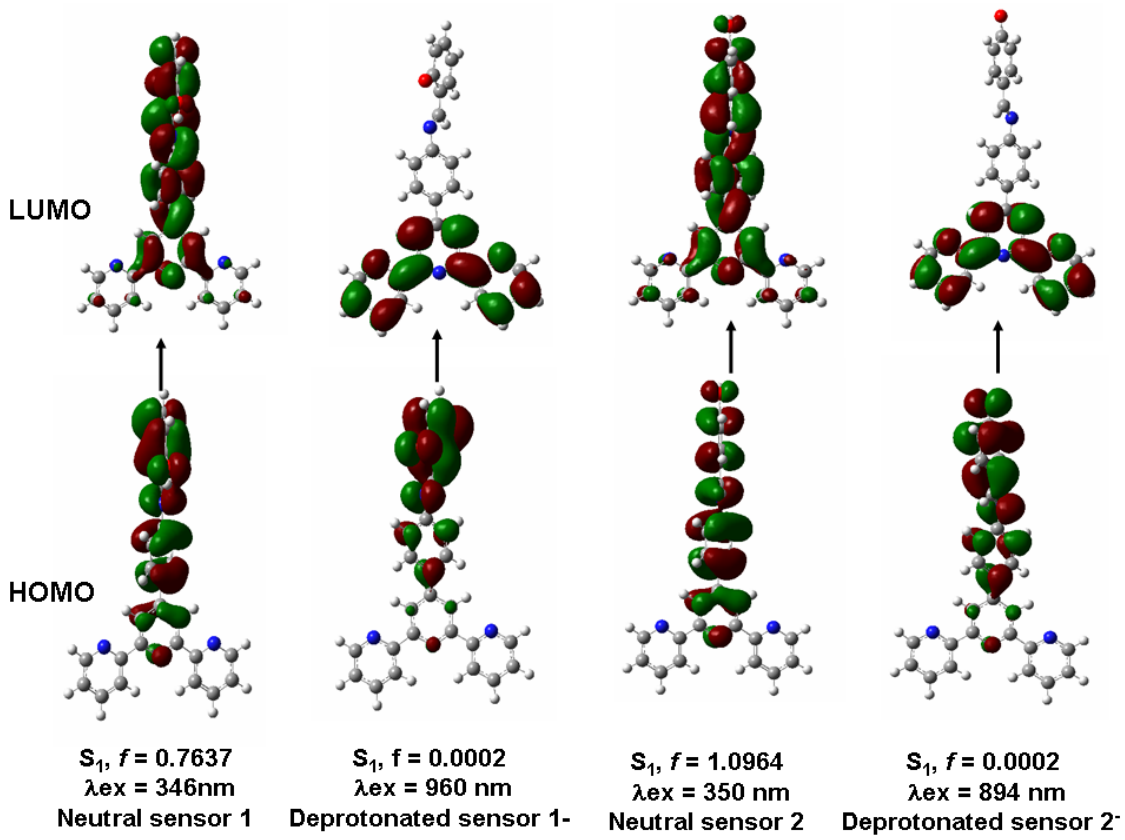

Fig. S8 Mechanism of the PET effect: HOMO and LUMO of neutral and deprotonated sensors **1** and **2**, calculated with DFT/TDDFT at the B3LYP/6-31G(d,p) level using Gaussian 09.

Table S1. Selected electronic excitation energies (eV) and oscillator strengths (*f*), configurations and CI coefficients of the low-lying electronically excited states of **1**, **2** and $\mathbf{1}^{-}$, $\mathbf{2}^{-}$.[a]

		TDDFT//B3LYP/6-31G(d,p)			
	Electronic transition	Energy(eV)[b]	*f*[c]	Composition[d]	CI[e]
	S0-S1	3.58(346nm)	0.7637	H→L	0.69300
	S0-S2	3.92(316nm)	0.0470	H→L+1	0.35077
				H−1→L	0.55008
1	S0-S3	3.95(313nm)	0.2475	H−2→L	0.66922
	S0-S4	4.11(302nm)	0.0362	H→L+1	0.57262
				H−1→L	0.39752
	S0-S9	4.48(277nm)	0.2626	H−1→L+1	0.64823
	S0-S1	1.29(960nm)	0.0002	H→L	0.70579
	S0-S2	1.45(857nm)	0.1841	H→L+1	0.70498
$\mathbf{1}^{-}$	S0-S3	1.89(656nm)	0.0116	H−1→L+1	0.67258
	S0-S4	1.90(654nm)	0.0002	H−1→L	0.70009
	S0-S8	2.60(476nm)	0.4988	H→L+4	0.69577
	S0-S1	3.54(350nm)	1.0964	H→L	0.67371
	S0-S2	3.80(326nm)	0.0131	H→L+1	0.59143
	S0-S3	4.01(309nm)	0.0521	H→L+2	0.56890
2	S0-S4	4.04(306nm)	0.1081	H→L+2	0.36381
				H−2→L	0.58414
	S0-S7	4.32(287nm)	0.3687	H→L+2	0.33508
				H−2→L	0.43815
	S0-S1	1.39(894nm)	0.0002	H→L	0.70587
	S0-S2	1.58(782nm)	0.2960	H→L+1	0.70303
$\mathbf{2}^{-}$	S0-S3	2.06(602nm)	0.0750	H→L+2	0.70297
	S0-S4	2.21(560nm)	0.0018	H→L+3	0.70629
	S0-S7	2.76(449nm)	0.9071	H→L+4	0.68748

[a]Calculated by TDDFT//B3LYP/6-31G(d,p), based on the DFT//B3LYP/6-31G(d,p) optimized ground state geometries. [b] Only the low-lying excited states and some allowed transitions were presented. [c] Oscillator strength. [d] H stands for HOMO and L stands for LUMO. Only the main configurations with configuration interaction (CI) coefficients > 0.3 are presented. [e] CI coefficients are in absolute values.

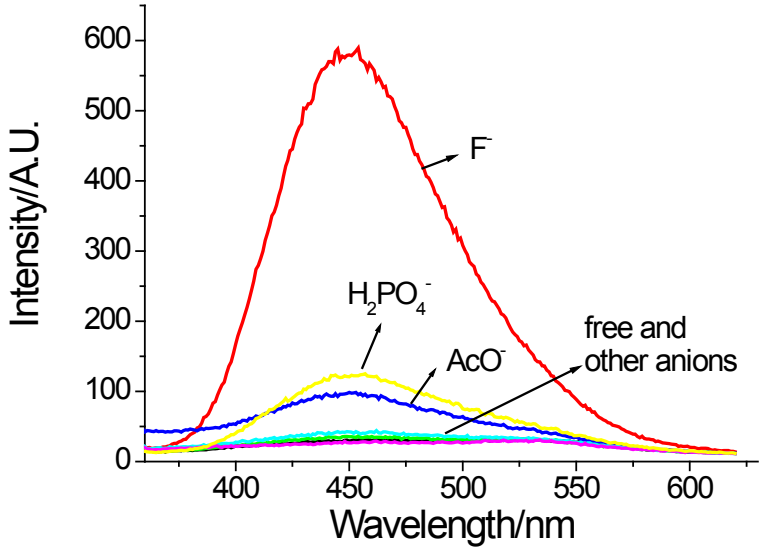

Fig. S9 Emission spectra of **1** upon the addition of F^- (6 equiv) and other anions (20 equiv) in CH_3CN solution (λ_{ex} = 330 nm).

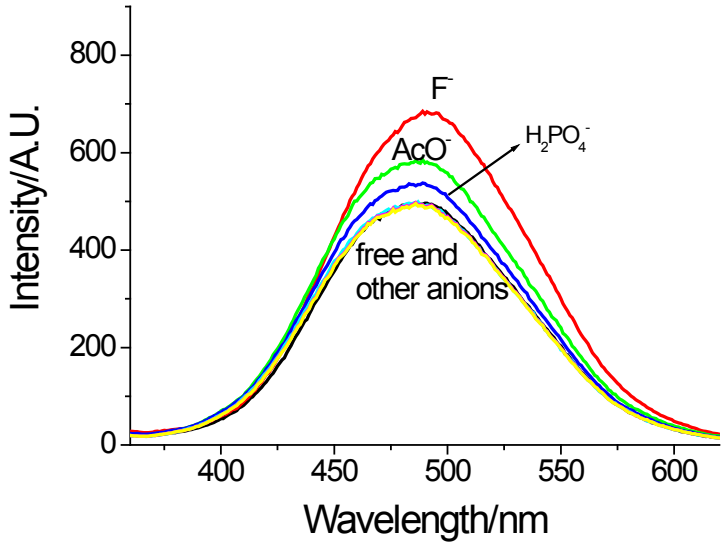

Fig. S10 Emission spectra of **2** upon the addition of F^- (6 equiv) and other anions (20 equiv) in CH_3CN solution (λ_{ex} = 330 nm).

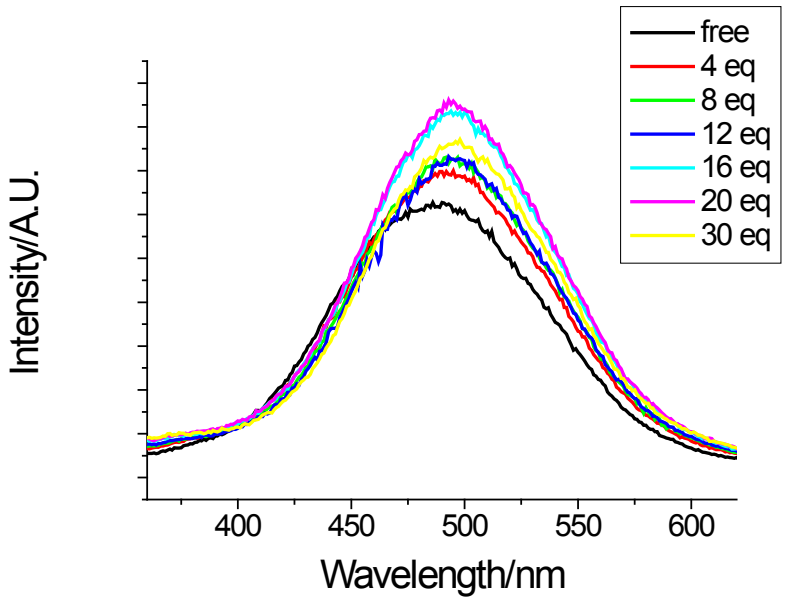

Fig. S11 Emission spectra of **2** upon the addition of CN^- (6 equiv) and other anions (20 equiv) in CH_3CN solution (λ_{ex} = 330 nm)

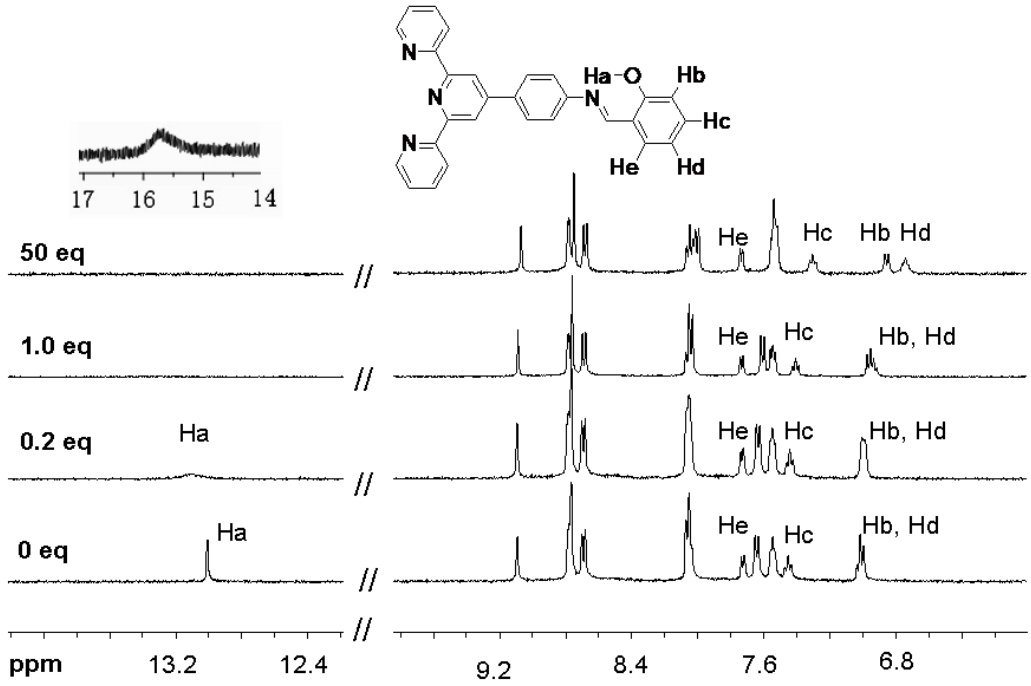

Fig. S12 ^1H NMR titration of **1** upon the addition of various amount of F^- in DMSO-d_6 solution

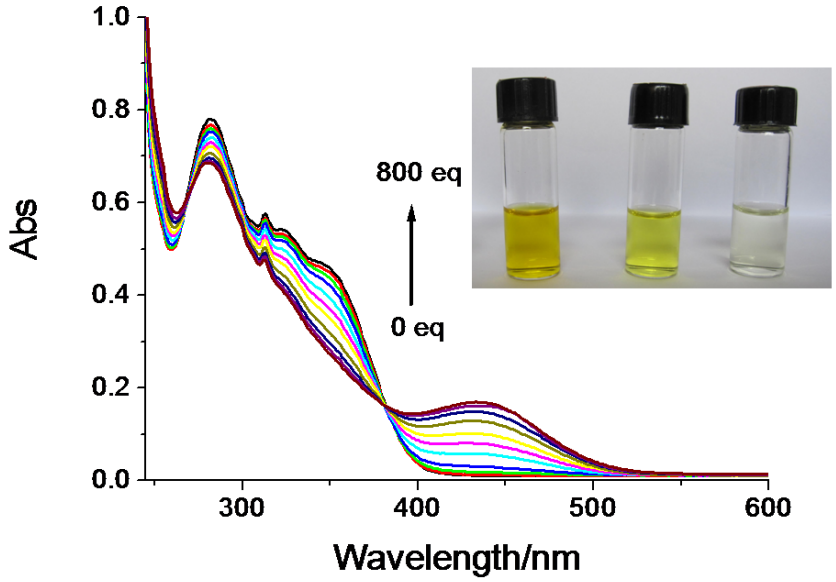

Fig S13 UV-vis spectra of **1** (2×10^{-5}M) upon the addition of 0-800 equiv of F^- in H_2O-CH_3CN (0.5:99.5, v/v) solution. Inset: form left to right, photograph of **1** (2×10^{-4}M) + 200 eq F^- in 100%, 95.5% and 1% aqueous CH_3CN solution.

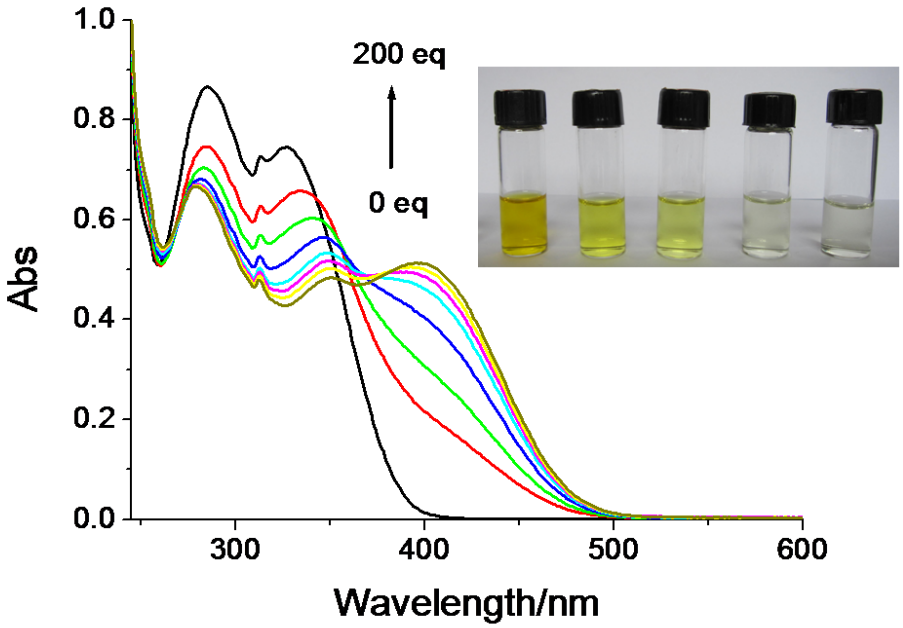

Fig S14 UV-vis spectra of **2** (2×10^{-5}M) upon the addition of 0-200 equiv of F^- in H_2O-CH_3CN (0.5:99.5, v/v) solution. Inset: form left to right, photograph of **2** (2×10^{-4}M) + 200 eq F^- in 100%, 95.5%, 1%, 2% and 5% aqueous CH_3CN solution.

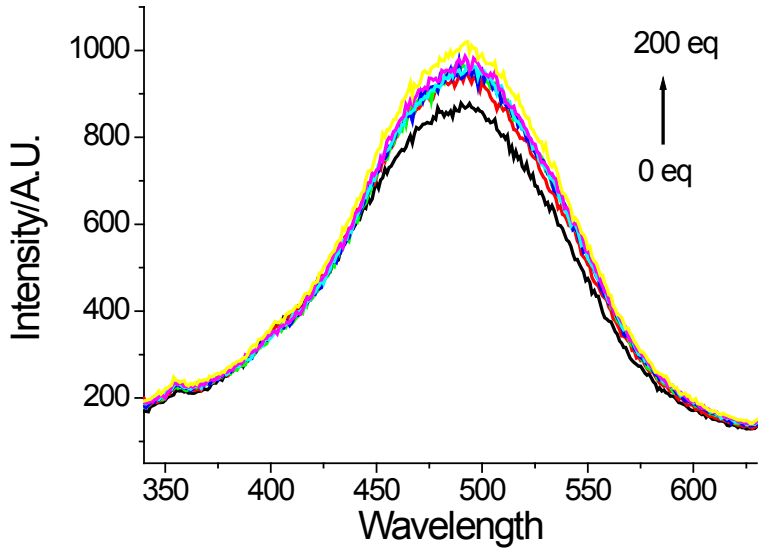

Fig S15 Emission spectra of **2** upon the addition of 0-200 equiv of F^- in H_2O/CH_3CN (1:99, V/V) solution (λ_{ex} = 330 nm)

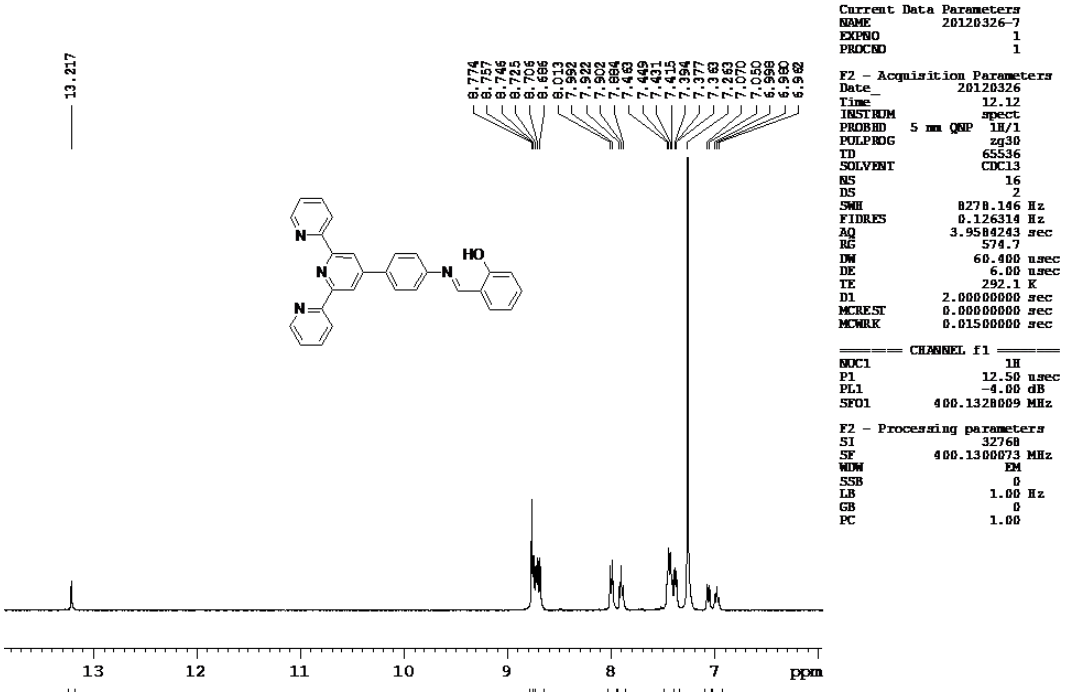

Fig. S16 ^1H NMR spectrum of **1** in $CDCl_3$

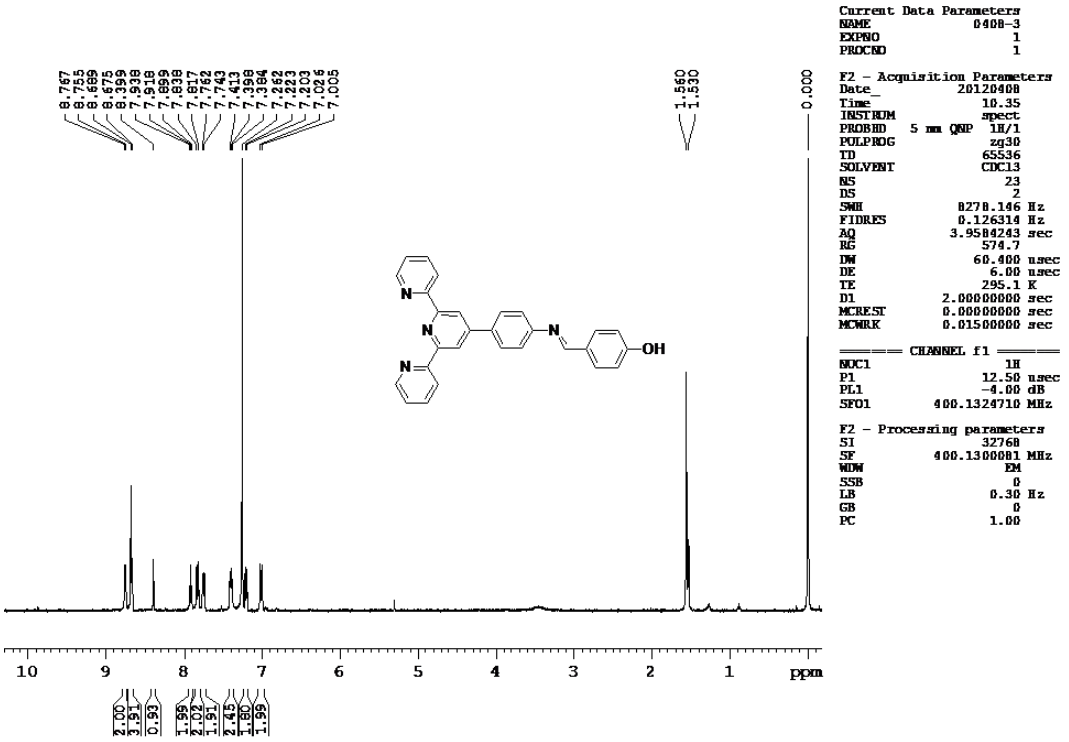

Fig. S17 ^{1}H NMR spectrum of **2** in $CDCl_3$

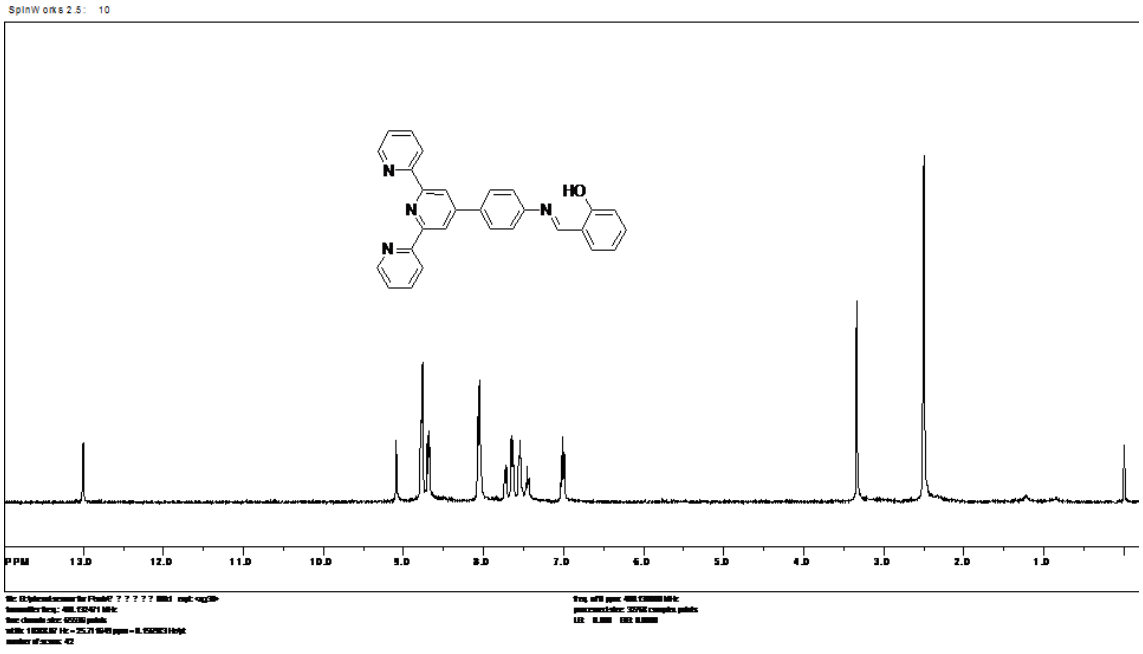

Fig. S18 ^{1}H NMR spectrum of **1** in DMSO-d_6

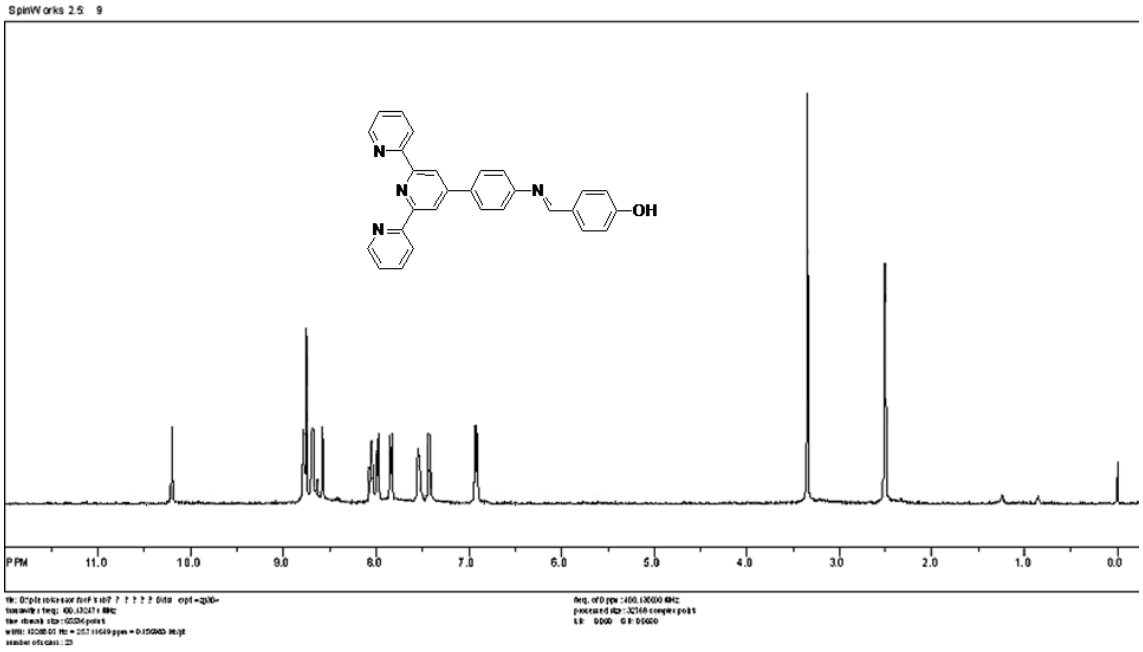

Fig. S19 ^{1}H NMR spectrum of **2** in DMSO-d_6

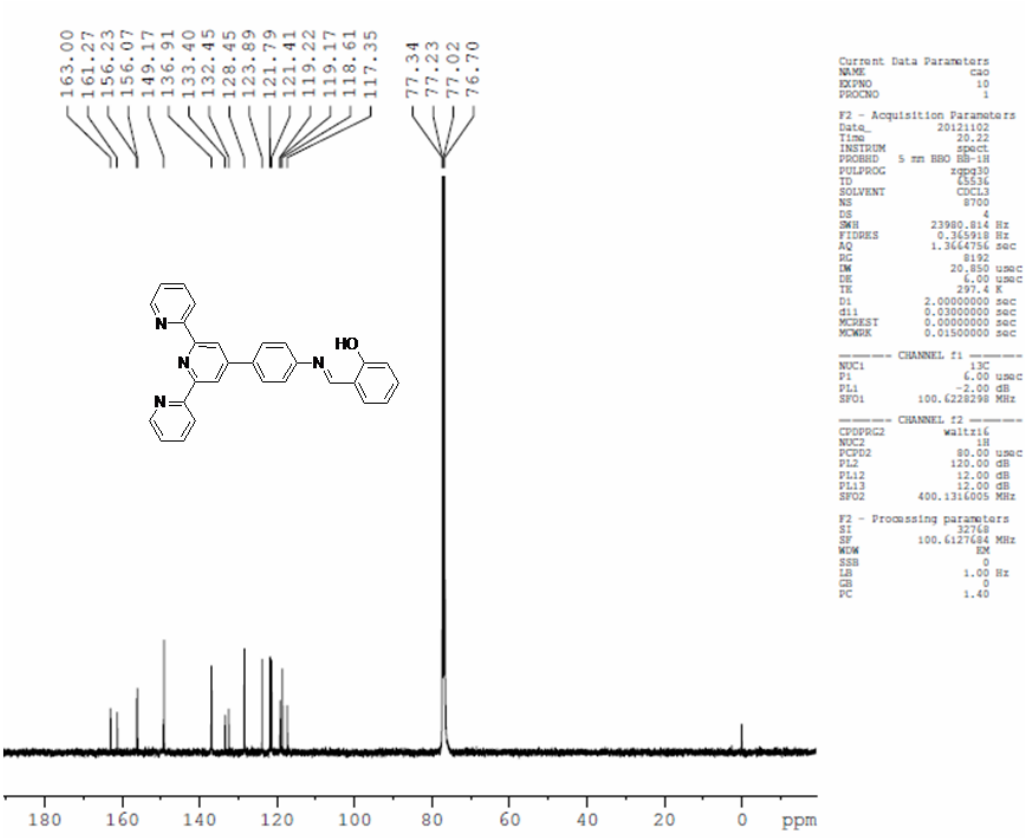

Fig. S20 ^{13}C NMR spectrum of **1** in $CDCl_3$

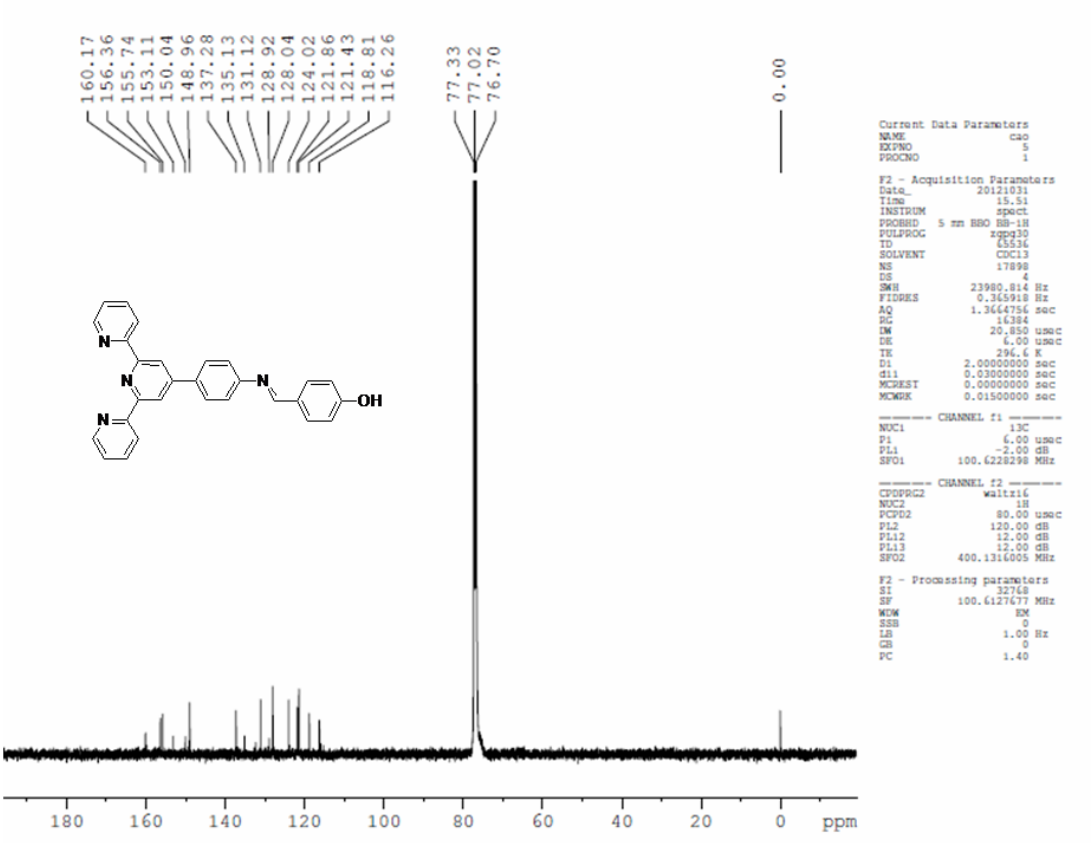

Fig. S21 ^{13}C NMR spectrum of **2** in $CDCl_3$

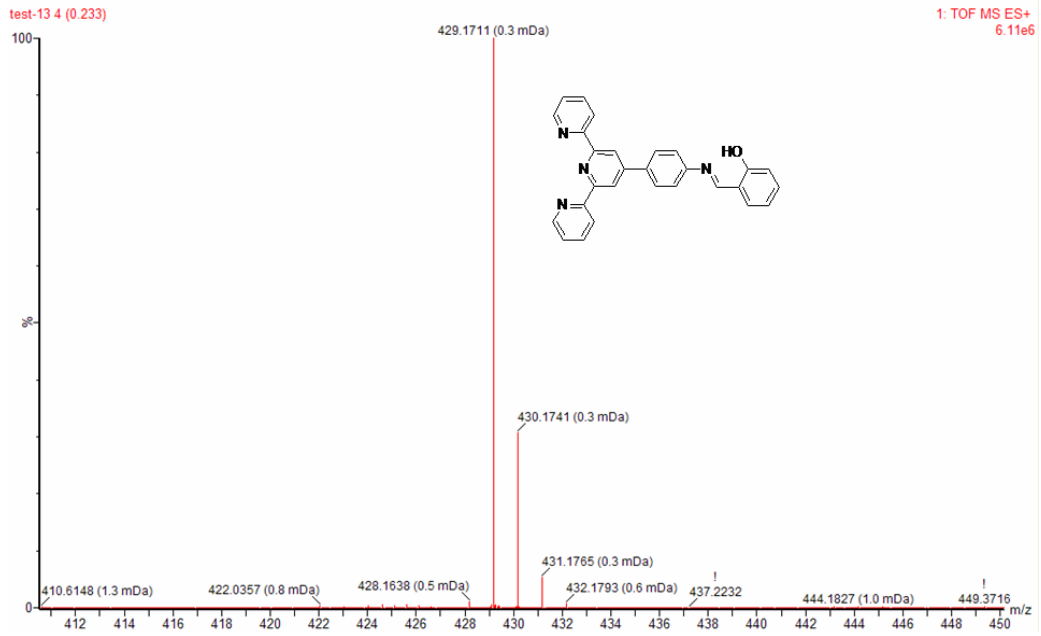

Fig. S22 HR-TOF-MS spectrum of **1**

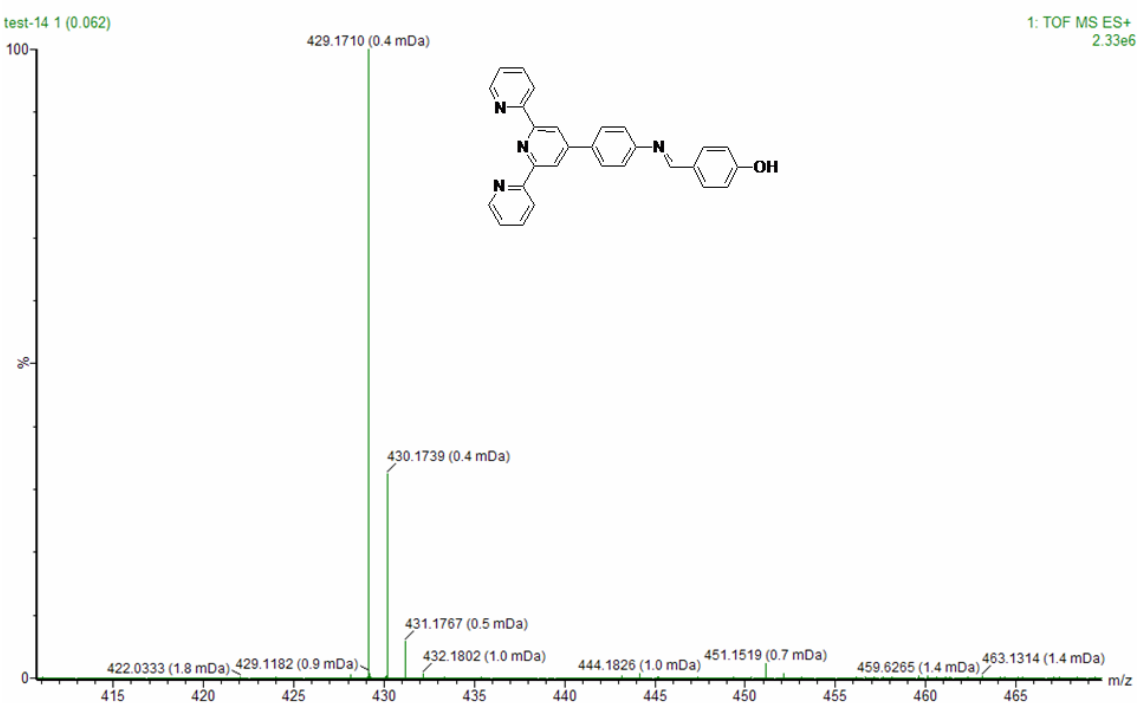

Fig. S23 HR-TOF-MS spectrum of **2**